Biosensors and Bioelectronics 278 (2025) 117309



Contents lists available at ScienceDirect

Biosensors and Bioelectronics

journal homepage: www.elsevier.com/locate/bios



ID-CRISPR: A CRISPR/Cas12a platform for label-free and sensitive detection of rare mutant alleles using self-interference DNA hydrogel reporter

Anni Deng [a,1], Zeyin Mao [a,1], Xiangyu Jin [a], Wenqi Lv [a], Leyang Huang [a], Hao Zhong [a], Shihong Wang [a], Yixuan Shi [a], Tianqi Zhou [c], Jianxin Zhao [a], Qin Huang [a], Xianbo Luo [e], Li Ma [e], Heng Zou [b,*], Rongxin Fu [c,d,**], Guoliang Huang [a,e,***]

[a] School of Biomedical Engineering, Tsinghua University, Beijing, 100084, China
[b] Department of Respiratory Medicine, Dongzhimen Hospital, Beijing University of Chinese Medicine, Beijing, China
[c] School of Medical Technology, Beijing Institute of Technology, Beijing, 100081, China
[d] Engineering Research Center of Integrated Acousto-opto-electronic Microsystems (Ministry of Education of China), Beijing Institute of Technology, Beijing, 100081, China
[e] National Engineering Research Center for Beijing Biochip Technology, Beijing, 102206, China

ARTICLE INFO

Keywords:
CRISPR/Cas12a
Hyperspectral interferometry
DNA hydrogel
Single nucleotide variant
EGFR L858R mutation
Non-small cell lung cancer

ABSTRACT

Accurate and sensitive detection of single nucleotide variants (SNVs) is paramount for cancer diagnosis and treatment. The CRISPR/Cas12a system shows promise for SNV detection due to its high sensitivity and single-base specificity. However, most CRISPR/Cas12a-based methods rely on F/Q-labeled single-stranded DNA (ssDNA) reporters, which are susceptible to fluorescence fluctuations, thereby reducing accuracy. To address these limitations, researchers have proposed using DNA hydrogels as signal transducers in CRISPR/Cas12a systems. Yet, the encapsulation of indicators into DNA hydrogels introduces additional instability, which could compromise both detection sensitivity and linearity. In this study, we integrated hyperspectral interferometry into a DNA hydrogel-based CRISPR/Cas12a detection platform (ID-CRISPR) to achieve sensitive label-free SNV detection. Using EGFR L858R SNV as a model target, we demonstrated that ID-CRISPR can detect mutant allele frequencies (MAFs) as low as 0.1% with a limit of detection (LOD) of 5 aM, while also showing its potential for quantifying SNV abundance. Its clinical utility was confirmed through analysis of lung tumor samples, with results consistent with sequencing data. Therefore, ID-CRISPR provides a sensitive, label-free, and user-friendly platform for SNV detection, offering new insights into combining optical sensing with DNA hydrogel technology in CRISPR/Cas assays.

1. Introduction

Accurate detection of single nucleotide variants (SNVs) is crucial for cancer early diagnosis and the guidance of tumor targeting drugs (Berger and Mardis, 2018). For instance, some SNVs of epidermal growth factor receptor (EGFR), like EGFR L858R, are critical predictors of the efficacy and sensitivity of EGFR-tyrosine kinase inhibitors (TKIs) in non-small cell lung cancer (NSCLC) patients (Lee et al., 2013). Current SNV detection methods include Sanger sequencing, next-generation sequencing (NGS), and polymerase chain reaction (PCR)-based approaches. Sanger sequencing requires >10% mutant allele presence and lacks sensitivity (Angulo et al., 2012). NGS is highly sensitive but time-consuming and necessitates complex bioinformatic analysis (Liu et al., 2021). PCR-based approaches demand precise primer design or advanced melting curve analysis for single-base specificity and high sensitivity (Bai et al., 2020; Chen et al., 2016). Therefore, a novel SNV detection method combining single-base specificity, high sensitivity, and user-friendliness is needed.

* Corresponding author.
** Corresponding author. School of Medical Technology, Beijing Institute of Technology, Beijing, 100081, China.
*** Corresponding author. School of Biomedical Engineering, Tsinghua University, Beijing, 100084, China.tshgl@mail.tsinghua.edu.cn
E-mail addresses: zouhang75@126.com (H. Zou), furongxin@bit.edu.cn (R. Fu).
[1] These authors contributed equally to this work.

https://doi.org/10.1016/j.bios.2025.117309
Received 24 December 2024; Received in revised form 16 February 2025; Accepted 23 February 2025
Available online 24 February 2025
0956-5663/© 2025 Published by Elsevier B.V.

In recent years, the clustered regularly interspaced short palindromic repeats (CRISPR) and CRISPR-associated (Cas) nuclease systems, a bacterial adaptive immune system against viral infections, have been increasingly utilized for SNV detection due to their excellent specificity (Broughton et al., 2020; Gong et al., 2021; Zeng et al., 2022). Cas12a, among the Cas proteins, stands out for its trans-cleavage activity, which enables efficient and indiscriminate cleavage of single-stranded DNA (ssDNA) following the targeting of double-stranded DNA (dsDNA) (Chen et al., 2018; Li et al., 2022; Zeng et al., 2021). Notably, most CRISPR/Cas12a-based detection systems are based on fluorophore F/Q-labeled ssDNA reporters that signal through fluorescence resonance energy transfer (FRET) (Li et al., 2018). While these reporters are user-friendly, they are prone to fluorescence fluctuations due to photobleaching, quenching, or the degradation of the ssDNA in the presence of nucleases in biological fluids (Liu et al., 2022; Uhlmann et al., 1997; Weng et al., 2023). Alternative reporters, including enzyme-labeled and spherical nucleic acid reporters, have been proposed, but they all necessitate complex modification or labeling processes (Chen et al., 2024; Fu et al., 2021; Li et al., 2020).

To address above limitations related to fluorescence fluctuations or complex labeling processes, researchers have proposed the use of DNA hydrogels as signal transducers in CRISPR/Cas12a detection systems (English et al., 2019). While these systems necessitate the encapsulation of various indicators—encompassing enzymes (Zhao et al., 2023), fluorescent dyes (Zhang et al., 2024), redox indicators (Zhang et al., 2024), and nanoparticles (Chen et al., 2022; Guo, J. et al., 2023; Zhang et al., 2024)—this encapsulation process can introduce instability, potentially degrading detection sensitivity and linearity, because the signal depends on the efficient release and diffusion of the indicators.

In this study, to eliminate the need for complex labeling or indicator encapsulation and thereby enable sensitive, label-free detection, we have innovatively integrated the optical sensing technique of hyperspectral interferometry into our DNA hydrogel-based CRISPR/Cas12a detection platform, which we have named ID-CRISPR. Using SNV of EGFR L858R for detection, we demonstrated that ID-CRISPR is capable of detecting mutant allele frequencies (MAFs) as low as 0.1%, with a limit of detection (LOD) reaching 5 aM, whereas NGS needs over 25,000 × sequencing depth for similar sensitivity, which is impractical for most patients (Song et al., 2021). ID-CRISPR not only offers enhanced sensitivity, specificity and user-friendliness, but also provides innovative insights into integrating optical sensing technology within CRISPR/Cas-based assays.

2. Materials and methods

2.1. Nucleic acid preparation

All oligonucleotides, including RPA primers, primers for DNA hydrogel preparation, and crRNAs were synthesized and purified by Sangon Biotech (Shanghai, China). The detailed sequences and modification were provided in Table S1. To prepare the wild-type and mutant fragments of EGFR L858R, we first extracted genomic DNAs from HeLa and H1975 cell lines using the DNeasy Blood & Tissue Kits (QIAGEN, Germany) with concentration determined by a Qubit 3 fluorometer (Invitrogen, Thermo Fisher Scientific, United States). Then we amplified the EGFR fragments through RPA, followed by purification using the FastPure Gel DNA Extraction Mini Kit (Vazyme, China).

To generate samples with varying MAFs, we prepared mixtures genomic DNAs of HeLa and H1975 cell lines in varying proportions at a total concentration of 50 fM. For instance, a sample with a 50% MAF was prepared by mixing equal volumes of genomic DNAs of HeLa and H1975 cell lines at 50 fM. The clinical tumor samples from 3 non-small cell lung cancer (NSCLC) patients were provided by Dongzhimen Hospital of Beijing University of Chinese Medicine under clinical ethical approval (2021DZMEC-164-02) from the medical ethics committee of the hospital. Genomic DNAs of tumor samples were extracted using the DNeasy Blood & Tissue Kits followed by RPA reaction for EGFR fragments amplification. The RPA products were sent to Sangon Biotech (Shanghai, China) for sequencing.

2.2. Principle of ID-CRISPR

As shown in Fig. 1A, there are mainly three steps for ID-CRISPR to achieve label-free SNV detection, which are ID-reporter-based CRISPR/Cas12a assay, hyperspectral interferometric detection, and spectrum analysis. In CRISPR/Cas12a assays, only when the Cas12a/crRNA complex recognizes the target DNA, the non-specific trans-cleavage activity of Cas12a can be activated. This activity leads to the degradation of the DNA hydrogel layer of ID-reporter. The reduction in the hydrogel layer's thickness correlates with the presence and abundance of the target sequence within Cas12a assay. After Cas12a assay, the thickness of the DNA hydrogel layer of ID-reporter is measured using hyperspectral interferometric detection and spectrum analysis. During hyperspectral interferometric detection, white light is reflected off both the top surface of the DNA hydrogel layer and the underlying silica-silicon interface, creating an interference pattern characterized by periodic oscillations. A decrease in the hydrogel layer's thickness shortens the optical path length, inducing a blue shift in the reflection spectrum. By analyzing and modeling the spectral data, the quantitative variation in thickness of the DNA hydrogel layer of ID-reporter can be calculated and used to report the target DNA.

2.3. Preparation and characterization of ID-Reporter

The ID-reporter was fabricated using a multi-step process on silicon wafers, involving thermal oxidation, primer immobilization, and DNA hydrogel formation based on RCA (Fig. 2A). Initially, silicon chips were oxidized to create a 900 nm thick silica layer (Tebo, Harbin, China), following by subsequent modification with amino groups, aldehyde groups and primers, according to the procedure established in previous work (Jin et al., 2022). In addition, the AT-rich circular DNA template (Circ-DNA) was prepared in advance for DNA hydrogel preparation with its preparation and characterization described in SI. Finally, the DNA hydrogel layer was prepared on the chip surface using a 10-h RCA reaction, according to an optimized protocol (SI) adapted from the literature (Yao et al., 2021; Zhao et al., 2023). Quality control measures were made to maintain consistent DNA hydrogel layer thickness across batches, which includes documenting reflection spectra to align with empirical benchmarks and monitoring the initial layer thickness. The dried ID-reporters can be stored in a sealed container at −20 °C for at least six months (data not shown), enabling long-term storage for subsequent use in CRISPR/Cas12a assays.

The ID-reporter was characterized with various methods, including macroscopic observation, fluorescence imaging, scanning electron microscope (SEM), contact angle measurements, and spectrum analysis. For fluorescence imaging, Cy3-labeled probes, which were complementary to Circ-DNA (Table S1), were hybridized onto the chips. The chips were then scanned using a confocal fluorescence scanner, LuxScan-10K/A (CapitalBio, Beijing, China). SEM images were captured using a FEI Quanta 200 Scanning Electron Microscope (FEI Inc, Netherlands) at 20 kV. Contact angles were measured using an OCA25 instrument (Dataphysics, Germany). Spectrum data was acquired using the optical setup described in the following section.

2.4. Hyperspectral interferometric detection and spectrum analysis

A hyperspectral interferometric system captured the ID-reporter's interference signal (Fig. 1B), using a halogen lamp's light (350–1000 nm) focused by lenses onto the ID-reporter. The reflected hyperspectral signal was directed through a lens and aperture to a spectrometer (Maya 2000 Pro, Ocean Optics, USA), recorded at 400 ms exposure.

This work characterizes the presence and quantification of the target

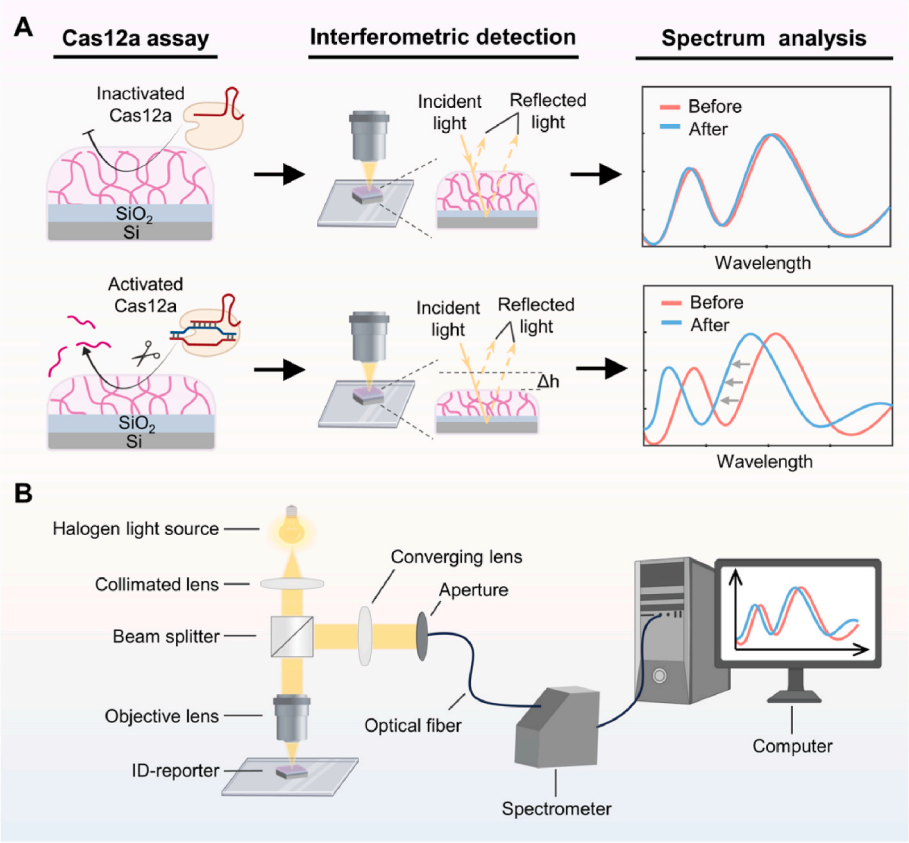


Fig. 1. Schematic illustration of the working principle of ID-CRISPR (A) and the setup of hyperspectral interferometric detection (B).

sequence by examining the nanoscale thickness changes of the DNA hydrogel on the silicon wafer. Upon broadband illumination striking the silicon wafer, a reflected light beam is generated from the DNA hydrogel surface, while a portion of the incident light traverses the hydrogel and the oxide layer of the silicon wafer, producing another reflected light at the silicon-silica interface. These two reflected beams, denoted as $U_1(\lambda)$ and $U_2(\lambda)$, lead to interference phenomena. The resulting reflectance spectrum, measured by the system, can be represented as follows:

$$R(\lambda) = \frac{U_1(\lambda)^2 + U_2(\lambda)^2 + 2U_1(\lambda)U_2(\lambda)\cos(4\pi nd/\lambda + 4\pi n_{DNA}h/\lambda_c)}{U(\lambda)^2} \quad (1)$$

Where d and h represent the thickness of the silicon oxide and DNA hydrogel layers, respectively; n and n_{DNA} are their average refractive indices; λ_c is the mean wavelength; and $U(\lambda)$ represents the illumination spectrum. Given that the theoretical values of n and n_{DNA} are similar in theory, the reflection between the hydrogel and oxide layer is negligible.

When the target sequence is present and amplified through the RPA process, the non-specific trans-cleavage activity of Cas12a is activated. Thus the hydrogel thickness on the silicon wafer decreases, leading to a nanoscale optical length change. The resulting reflectance spectrum is then expressed as:

$$R'(\lambda) = \frac{U_1(\lambda)^2 + U_2(\lambda)^2 + 2U_1(\lambda)U_2(\lambda)\cos[4\pi nd/\lambda + 4\pi n_{DNA}(h - \Delta h)/\lambda_c]}{U(\lambda)^2} \quad (2)$$

The optical path difference $\Delta = 2n_{DNA}\Delta h$ is used for spectral calculations, which provides a quantitative sensing result. The reflectance spectrum follows a trigonometric function form. Using a Fourier transform method, we analyze the optical path difference before and after the reaction. We apply the Fourier transform to $R(\lambda)$-$R'(\lambda)$ along the wavenumber $2\pi/\lambda$ axis, extracting the phase at the peak m with the highest amplitude in the transformed result, and multiply it by λ_c to obtain the final value:

$$\Delta = \lambda_c \times \text{Phase}\{\text{FFT}[R(\lambda) - R'(\lambda)], m\} \quad (3)$$

where FFT(*) is the fast Fourier transform operator, and Phase(*, m) is the phase at index m of the FFT result.

2.5. CRISPR/Cas12a assays for nucleic acid detection

The Cas12a assay was performed according to the literature and the instructions of the manufacture of LbCas12a (NEB, United Kingdom) with some modifications (Zhao et al., 2023). First, the nucleic acid sample underwent a 20-min RPA reaction using the TwistAmp Basic Kit (TwistDx, United Kingdom) as detailed in SI. Then, a Cas12a reaction mixture with a total volume of 20 μL was prepared, comprising LbCas12a (100 nM), crRNA (50 nM), 1X NEBuffer r2.1, and 1 μL of the RPA products. Finally, the RPA products and an ID-reporter or FQ-ssDNA reporter (500 nM) were added to the Cas12a reaction mixture and then incubated at 45 °C for 1 h.

3. Results and discussion

3.1. Preparation and characterization of the ID-reporter

The DNA hydrogel layer of ID-reporter grow on a solid surface and form a thin layer through the RCA reaction, where an AT-rich Circ-DNA was amplified from the primer immobilized on the chip surface with the involvement of phi29 DNA polymerase (Qiu et al., 2017; Zhang et al., 2018). Unlike DNA hydrogel used for indicator encapsulation, which require a rigid structure, our hydrogel layer for interferometry does not need such a rigid structure but demands better optical transparency. To achieve this, we reduced the RCA reaction time from 20 h to 10 h

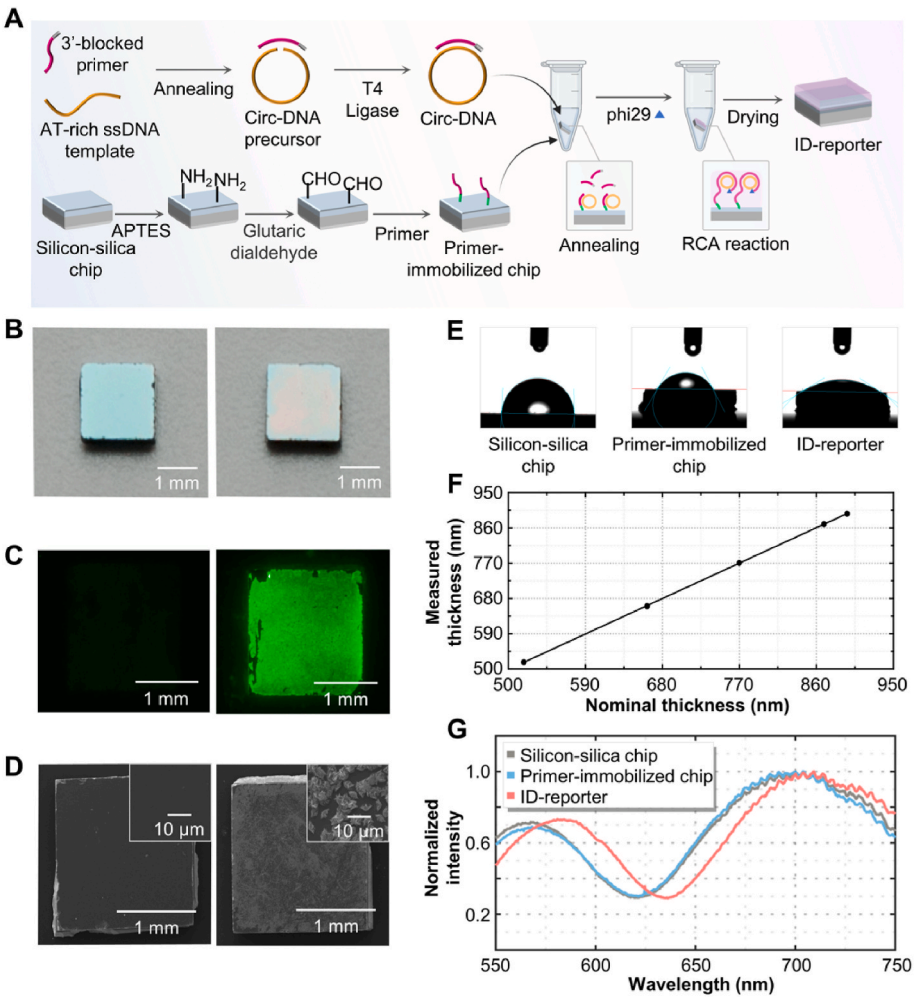


Fig. 2. (A) Schematic illustration of the preparation of ID-reporter. (B–D) Macroscopic observations, fluorescence images, and SEM images of the primer-immobilized chip (left) and the ID-reporter (right). (E) Contact angle measurements. (F) The results of measuring the thickness of different silica layers using hyperspectral interferometry. (G) The reflection spectrum analysis.

(Fig. S2) (Zhang et al., 2024; Zhao et al., 2023).

As shown in Fig. 2B, the ID-reporter visually exhibited a colorful reflection distinct from the primer-immobilized chip, likely due to the distinct refractive indices of the DNA hydrogel and silica layers. Fluorescent probe hybridization (Fig. 2C) further confirmed the DNA hydrogel layer's formation, with the ID-reporter showing markedly increased fluorescence signals. SEM imaging (Fig. 2D) revealed the uniform flower-like DNA hydrogel microstructures on ID-reporter's surface, consistent with previous studies (Huang et al., 2017; Lee et al., 2012). Contact angle measurements (Fig. 2E) revealed that the hydrophilicity of DNA hydrogel layer changed the physicochemical properties of the chip surface. The ID-reporter exhibited a contact angle of 33.57 ± 1.17°, significantly smaller than that of the silicon-silica chip (90.35 ± 2.70°) and primer-immobilized chip (59.74 ± 4.75°).

In addition, we used hyperspectral interferometry to characterize the ID-reporter after evaluating the performance of hyperspectral interferometric detection. Silicon wafers with varying nominal thicknesses of silica layers were employed to evaluate the detection sensitivity. The detection results are shown in Fig. 2F, with a maximum standard deviation of 0.43 nm, highlighting the high quantitative accuracy of this detection method. The detailed measured results are listed in Table S2. Subsequently, we acquired hyperspectral interferometric spectra from chips with different modification, including the ID-reporter. Fig. 2G illustrates that, in comparison to other chips, a significant redshift was observed in the ID-reporter's reflection spectrum, attributed to the formation of a DNA hydrogel layer on the chip surface.

3.2. *Verification of the ID-reporter for hyperspectral interferometric CRISPR/Cas12a detection*

To further confirm the feasibility of ID-CRISPR for detection of mutant alleles, we initially designed a crRNA specifically targeting the EGFR mutation, as depicted in Fig. 3A. Given that single-base detection specificity relies heavily on crRNA design, we introduced one additional mismatch near the PAM sequence (TTTV) and the mutant site, based on previous findings (Dai et al., 2019; Meng et al., 2021; Zhang et al., 2023). We designed six crRNAs with one additional mismatch positioned 1 or 2 nucleotides upstream of the mutation site as described in Table S3. Among these, crRNA-2 exhibited the highest specificity in FQ-ssDNA reporter-based real-time CRISPR/Cas12a assays (Fig. 3B and Fig. S3) and was thus selected for further analysis. Capillary electrophoresis was then used to analyze the endpoint products of the ID-reporter-based CRISPR/Cas12a assays (Fig. S4). Notably, the mutation targeted in this study is located near the PAM sequence. For PAM-free SNV detection, recent studies have demonstrated the potential of introducing a PAM sequence near the target mutation site through PCR primer design(Chen et al., 2021). Our method can be integrated with similar strategies to enable the detection of any mutation without dependence on an adjacent PAM sequence.

Then, as shown in Fig. 3C, we further demonstrated the cleavability

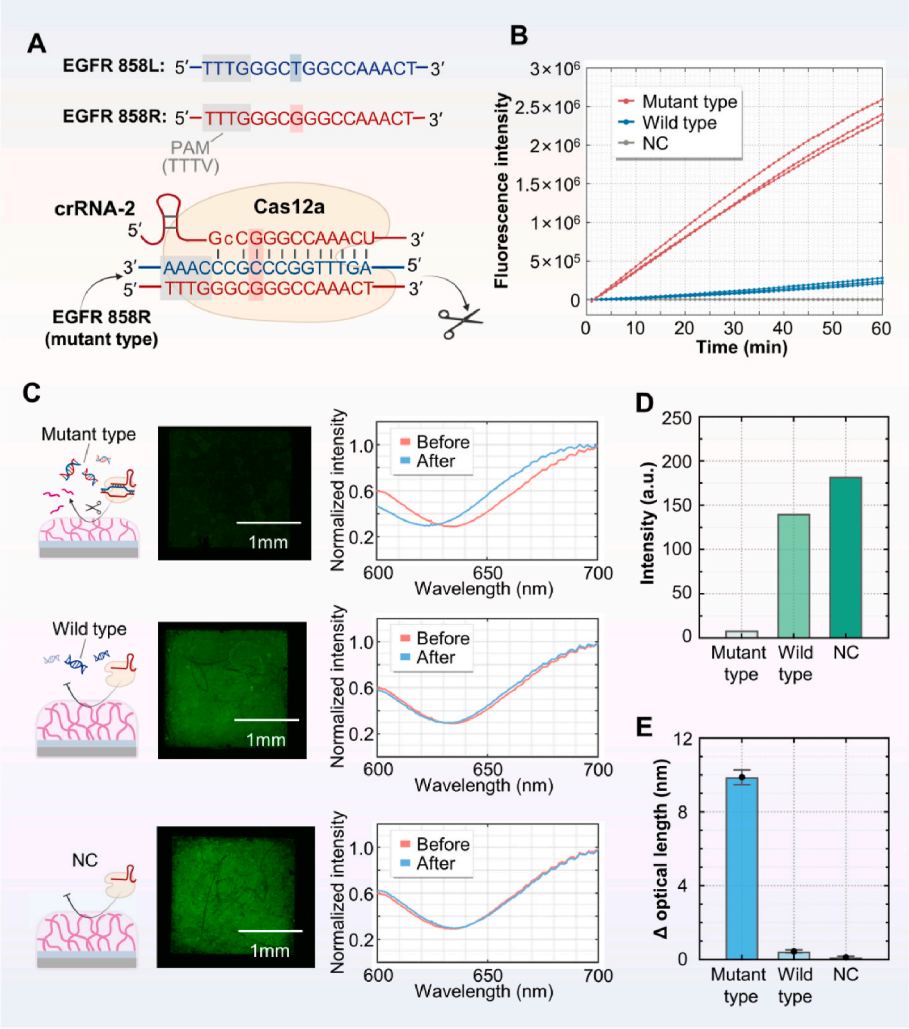


Fig. 3. (A) EGFR L858R wild-type and mutant sequences with a crRNA designed to target the EGFR L858R mutation. (B) Specificity validation of crRNA-2 targeting EGFR L858R mutant via FQ-ssDNA reporter-based realtime CRISPR/Cas12a assays. (C) Schematic (left), fluorescent probe hybridization (middle), and reflection spectra (right) of ID-reporters subjected to CRISPR/Cas12a assays with EGFR L858R mutant, wild type, and NC (water). (D) Statistical analysis of fluorescent probe hybridization and (E) reflection spectrum analysis.

of DNA hydrogel layer of the ID-reporter and its spectral distinguishability. To assess the cleavability of DNA hydrogel, we conducted fluorescent probe hybridization on ID-reporters subjected to CRISPR/Cas12a assays with various samples, including the EGFR L858R mutant and wild type at a concentration of 50 fM, and water as a negative control. The designed crRNA-2 recognized the EGFR L858R mutant specifically, activating Cas12a's trans-cleavage activity and leading to the degradation of the ID-reporter's DNA hydrogel layer. As anticipated, the statistical analysis of fluorescence intensity (Fig. 3D) demonstrated that the ID-reporter treated with the mutant type exhibited a significantly reduced fluorescent signal (8.75 a.u.) compared to the wild type (140.38 a.u.) and water (182.26 a.u.), indicative of enzymatic cleavage of the DNA hydrogel layer.

Furthermore, the cleavage of the DNA hydrogel in the ID-reporter was observable in the reflection spectrum as a blue shift. Through further analysis of this spectral shift, we calculated the optical path length reductions for the ID-reporter treated with the mutant type, wild type, and water (NC) to be 9.88 ± 0.40, 0.45 ± 0.08, and 0.13 ± 0.05 nm, respectively (Fig. 3E). Therefore, above results confirm the cleavability of the DNA hydrogel and the ability to distinguish between cleaved and uncleaved ID-reporters using hyperspectral interferometric detection, thereby validating the ID-CRISPR principle's feasibility.

3.3. Performance analysis of ID-CRISPR in detecting rare mutations

It is crucial for SNV detection systems to effectively identify mutations in the heterogeneous genomic DNA samples. Therefore, ID-CRISPR's selectivity and sensitivity were evaluated using mock samples, as depicted in Fig. 4A. The selectivity assessment involved testing ID-CRISPR with mock samples featuring varying MAFs: 0%, 0.1%, 1%, 5%, 10%, 50%, and 100%, each at a concentration of 50 fM. The corresponding changes in optical length for these samples were 0.39 ± 0.09, 0.97 ± 0.04, 1.55 ± 0.47, 4.48 ± 0.52, 5.52 ± 0.22, 8.26 ± 0.38, and 10.96 ± 0.89 nm, respectively, with a negative control (water) yielding a value of 0.18 ± 0.07 nm (Fig. 4B). Furthermore, the analytical sensitivity of ID-CRISPR was evaluated with mock samples containing the EGFR L858R mutation across a concentration gradient from 5 aM to 50 fM. As shown in Fig. 4C, there is a proportional increase in the change of optical length as the concentration increases with a good linear relationship ($R^2 = 0.936$), which suggests the quantitative potential of ID-CRISPR. ID-CRISPR demonstrated superior sensitivity and specificity compared to the FQ-ssDNA reporter-based CRISPR system, capable of detecting MAFs down to 0.1% and achieving a LOD as low as 5 aM, whereas the FQ-ssDNA reporter-based system can detect MAFs of 1 % with a LOD of 50 aM (Fig. S5).

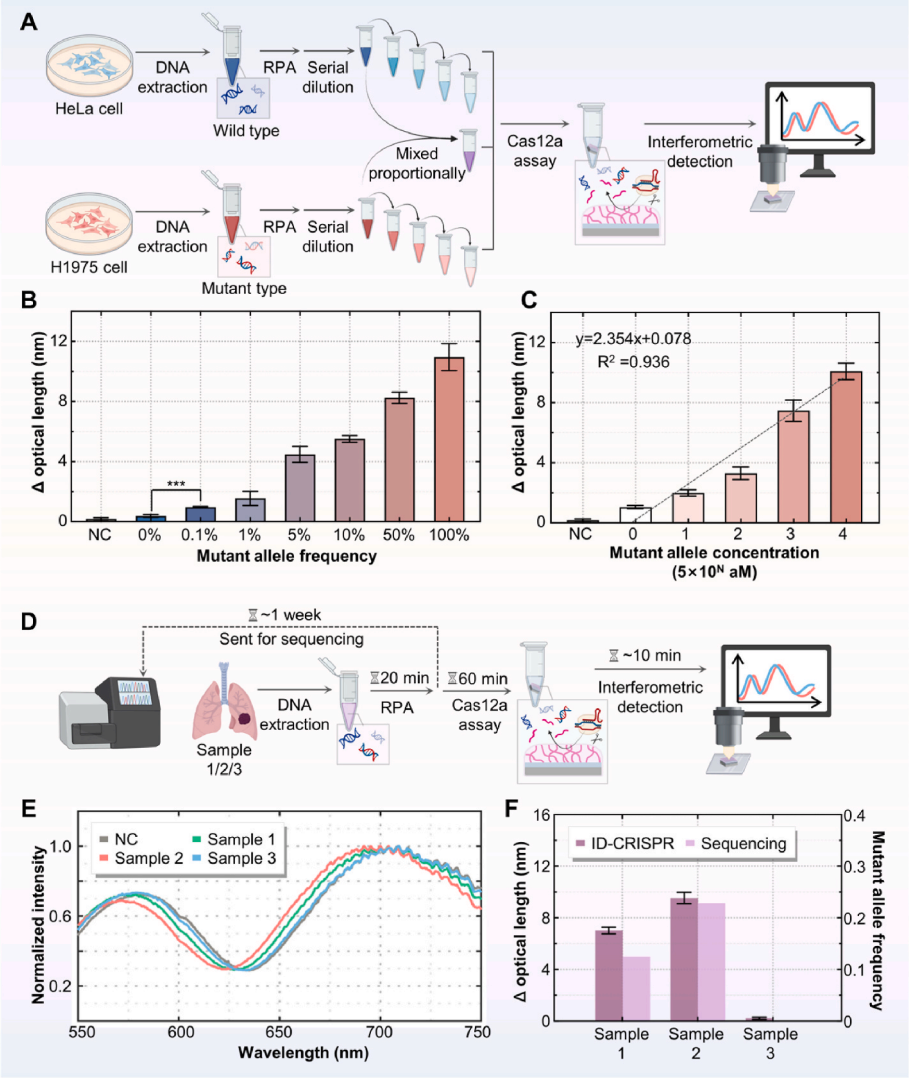


Fig. 4. (A) Schematic workflow of assessing ID-CRISPR's analytical selectivity and sensitivity in detecting the EGFR L858R mutant using mock samples. (B) Selectivity assessment of ID-CRISPR using mock samples across various MAFs. (C) Sensitivity assessment of ID-CRISPR with mock samples containing EGFR L858R mutation at varying concentrations. (D) Schematic workflow for clinical sample detection using ID-CRISPR and sequencing. (E) Reflection spectra from ID-CRISPR detection of clinical samples. (F) Comparison of clinical sample detection results between ID-CRISPR and sequencing. NC, negative control.

3.4. Validation of ID-CRISPR using clinical samples

Finally, we assessed the clinical applicability of ID-CRISPR by analyzing three tissue samples obtained from lung cancer patients, with the EGFR L858R mutation abundance determined by sequencing. As depicted in Fig. 4D, after DNA extraction and RPA reactions, each sample was divided into two aliquots. One aliquot underwent ID-CRISPR detection and analysis; and the other was sent to high-throughput sequencing to determine the presence and abundance of EGFR L858R mutations. The spectrum results of sample 1 and sample 2 exhibited a blue shift (Fig. 4E), indicating DNA hydrogel degradation by Cas12a's trans-cleavage. Optical length decreases were calculated using our algorithm based on the spectral changes and then compared with MAFs determined by sequencing (Fig. 4F). Sample 1 and Sample 2, with MAFs of 12.51% and 22.84%, respectively, exhibited decreases in optical length of 7.03 ± 0.25 nm and 9.54 ± 0.43 nm. In contrast, Sample 3, with an remarkably low MAF of 0.09% and a negative mutation diagnosis, exhibited a minimal decrease of 0.23 ± 0.08 nm, which was indistinguishable from the negative control. These results confirm the concordance between our ID-CRISPR results and sequencing data, in terms of both mutation presence and quantity. However, the current sample size is limited, requiring validation with a larger cohort of samples in the future.

4. Conclusion

In conclusion, we have proposed a novel SNV detection platform named ID-CRISPR, which innovatively integrated hyperspectral interferometry and DNA hydrogel to achieve sensitive label-free detection. Demonstrated through the detection of the EGFR L858R SNV, ID-CRISPR combined with RPA is capable of detecting SNV down to the attomolar molecular weight level (5 aM) and MAFs as low as 0.1%. Its clinical practicability was confirmed using lung tumor samples, with results consistent with gold-standard sequencing (Jr and Bardelli, 2014). Compared with other detection strategies for EGFR mutations (Table S4), ID-CRISPR outperforms fluorescence-based methods in selectivity and sensitivity by employing DNA hydrogel as signal reporters, thereby circumventing fluorescence fluctuations; it surpasses electrochemistry-based methods in detection speed and user-friendliness by eliminating the need for complex labeling processes.

Although our platform achieved high sensitivity, selectivity, and ease of use in detecting rare mutant alleles, there are areas where ID-CRISPR

can be further improved. Currently, the high sensitivity of the assay necessitates separate RPA reactions for preamplification, which increases the risk of aerosol-induced contamination. Future iterations could integrate sample processing and preamplification steps, enabling a more reliable and integrated detection system (Mao et al., 2024; Wu et al., 2021; Zhou et al., 2024). Additionally, ID-CRISPR's multiplex analysis ability should be expanded to enhance its clinical application value, which could be achieved by incorporating orthogonal Cas enzymes (Gootenberg et al., 2018), introducing partitions in DNA hydrogel chips (Guo et al., 2023), or utilizing microfluidics (Bruch et al., 2021; Li et al., 2024).

CRediT authorship contribution statement

Anni Deng: Writing – original draft, Conceptualization. **Zeyin Mao:** Methodology, Conceptualization. **Xiangyu Jin:** Formal analysis, Conceptualization. **Wenqi Lv:** Resources, Project administration, Conceptualization. **Leyang Huang:** Resources, Data curation. **Hao Zhong:** Writing – review & editing, Formal analysis. **Shihong Wang:** Writing – review & editing, Resources. **Yixuan Shi:** Resources. **Tianqi Zhou:** Resources, Data curation. **Jianxin Zhao:** Resources. **Qin Huang:** Resources. **Xianbo Luo:** Resources, Project administration. **Li Ma:** Supervision, Resources. **Heng Zou:** Resources, Project administration. **Rongxin Fu:** Writing – review & editing, Project administration, Methodology. **Guoliang Huang:** Writing – review & editing, Supervision, Project administration, Funding acquisition.

Declaration of competing interest

The authors declare that they have no known competing financial interests or personal relationships that could have appeared to influence the work reported in this paper.

Acknowledgments

This study was funded by the National Key Research and Development Program of China (2023YFF0721501 and 2018YFA0704000), the National Natural Science Foundation of China (62375148, 61927819, 81827808 and 62105177), the Sichuan Science and Technology Program (2021YFQ0060 and 2022YFS0637), Young Elite Scientists Sponsorship Program by CAST (2023QNRC001), Natural Science Foundation of Chongqing (2024NSCQ-MSX3784), Vanke Special Fund for Public Health and Health Discipline Development, Tsinghua University (2022Z82WKJ002), the Tsinghua University Spring Breeze Fund (2020Z99CFG011), the Beijing Lab Fundation and Tsinghua SRT innovation Fund (2411T0725, 2411T0728), and Tsinghua Laboratory Innovation Fund (100020019), State Key Laboratory of Optoelectronic Materials and Technologies (Sun Yat-sen University, OEMT-2024- KF-03).

Appendix A. Supplementary data

Supplementary data to this article can be found online at https://doi.org/10.1016/j.bios.2025.117309.

Data availability

Data will be made available on request.

References

Angulo, B., Conde, E., Suárez-Gauthier, A., Plaza, C., Martínez, R., Redondo, P., Izquierdo, E., Rubio-Viqueira, B., Paz-Ares, L., Hidalgo, M., López-Ríos, F., 2012. A comparison of EGFR mutation testing methods in lung carcinoma: direct sequencing, real-time PCR and immunohistochemistry. PLoS One 7 (8), e43842.

Bai, S.L., Xu, B.T., Zhang, Y.L., Zhang, Y.H., Dang, H., Yang, S.S., Zuo, C., Zhang, L., Li, J. J., Xie, G.M., 2020. Tuning the specificity of DNA probes using bulge-loops for low-abundance SNV detection. Biosens. Bioelectron. 154, 112092.

Berger, M.F., Mardis, E.R., 2018. The emerging clinical relevance of genomics in cancer medicine. Nat. Rev. Clin. Oncol. 15 (6), 353–365.

Broughton, J.P., Deng, X., Yu, G., Fasching, C.L., Servellita, V., Singh, J., Miao, X., Streithorst, J.A., Granados, A., Sotomayor-Gonzalez, A., 2020. CRISPR–Cas12-based detection of SARS-CoV-2. Nat. Biotechnol. 38 (7), 870–874.

Bruch, R., Johnston, M., Kling, A., Mattmüller, T., Baaske, J., Partel, S., Madlener, S., Weber, W., Urban, G.A., Dincer, C., 2021. CRISPR-powered electrochemical microfluidic multiplexed biosensor for target amplification-free miRNA diagnostics. Biosens. Bioelectron. 177, 112887.

Chen, H., Feng, Y., Liu, F., Tan, C., Xu, N., Jiang, Y., Tan, Y., 2024. Universal smartphone-assisted label-free CRISPR/Cas12a-DNAzyme chemiluminescence biosensing platform for on-site detection of nucleic acid and non-nucleic acid targets. Biosens. Bioelectron. 247, 115929.

Chen, J.S., Ma, E., Harrington, L.B., Da Costa, M., Tian, X., Palefsky, J.M., Doudna, J.A., 2018. CRISPR-Cas12a target binding unleashes indiscriminate single-stranded DNase activity. Science 360 (6387), 436–439.

Chen, M., Zhang, J., Peng, Y., Bai, J., Li, S., Han, D., Ren, S., Qin, K., Zhou, H., Han, T., Wang, Y., Gao, Z., 2022. Design and synthesis of DNA hydrogel based on EXPAR and CRISPR/Cas14a for ultrasensitive detection of creatine kinase MB. Biosens. Bioelectron. 218.

Chen, T., Jia, Y., Dong, C., Gao, J., Mak, P.I., Martins, R.P., 2016. Sub-7-second genotyping of single-nucleotide polymorphism by high-resolution melting curve analysis on a thermal digital microfluidic device. Lab Chip 16 (4), 743–752.

Chen, Y., Mei, Y., Jiang, X., 2021. Universal and high-fidelity DNA single nucleotide polymorphism detection based on a CRISPR/Cas12a biochip. Chem. Sci. 12 (12), 4455–4462.

Dai, Y., Somoza, R.A., Wang, L., Welter, J.F., Li, Y., Caplan, A.I., Liu, C.C., 2019. Exploring the trans-cleavage activity of CRISPR-cas12a (cpf1) for the development of a universal electrochemical biosensor. Angew. Chem. Int. Ed. 58 (48), 17399–17405.

English, M.A., Soenksen, L.R., Gayet, R.V., de Puig, H., Angenent-Mari, N.M., Mao, A.S., Nguyen, P.Q., Collins, J.J., 2019. Programmable CRISPR-responsive smart materials. Science 365 (6455), 780–785.

Fu, X., Shi, Y., Peng, F., Zhou, M., Yin, Y., Tan, Y., Chen, M., Yin, X., Ke, G., Zhang, X.-B., 2021. Exploring the trans-cleavage activity of CRISPR/Cas12a on gold nanoparticles for stable and sensitive biosensing. Anal. Chem. 93 (11), 4967–4974.

Gong, H., Wu, Y., Zeng, R., Zeng, Y., Liu, X., Tang, D., 2021. CRISPR/Cas12a-mediated liposome-amplified strategy for the photoelectrochemical detection of nucleic acid. Chem. Commun. 57 (71), 8977–8980.

Gootenberg, J.S., Abudayyeh, O.O., Kellner, M.J., Joung, J., Collins, J.J., Zhang, F., 2018. Multiplexed and portable nucleic acid detection platform with Cas13, Cas12a, and Csm6. Science 360 (6387), 439–444.

Guo, J., Zhu, Y., Miao, P., 2023. Nano-impact electrochemical biosensing based on a CRISPR-responsive DNA hydrogel. Nano Lett. 23 (23), 11099–11104.

Guo, Y., Li, W.X., Zhang, R.C., Cao, S.Y., Zhu, X.L., Chen, G.F., Feng, C., 2023. A portable and partitioned DNA hydrogel chip for multitarget detection. Lab Chip 23 (11), 2601–2610.

Huang, Y., Xu, W., Liu, G., Tian, L., 2017. A pure DNA hydrogel with stable catalytic ability produced by one-step rolling circle amplification. Chem. Commun. 53 (21), 3038–3041.

Jin, X.Y., Fu, R.X., Du, W.L., Shan, X.H., Mao, Z.Y., Deng, A.N., Lin, X., Su, Y., Yang, H., Lv, W.Q., Zhong, H., Huang, G.L., 2022. Rapid, highly sensitive, and label-free pathogen assay system using a solid-phase self-interference recombinase polymerase amplification chip and hyperspectral interferometry. Anal. Chem. 94 (6), 2926–2933.

Jr, L.A.D., Bardelli, A., 2014. Liquid biopsies: genotyping circulating tumor DNA. J. Clin. Oncol. 32 (6), 579–586.

Lee, C.K., Brown, C., Gralla, R.J., Hirsh, V., Thongprasert, S., Tsai, C.-M., Tan, E.H., Ho, J.C.-M., Chu, D.T., Zaatar, A., 2013. Impact of EGFR inhibitor in non–small cell lung cancer on progression-free and overall survival: a meta-analysis. J. Natl. Cancer Inst. 105 (9), 595–605.

Lee, J., Peng, S.M., Yang, D.Y., Roh, Y.H., Funabashi, H., Park, N., Rice, E.J., Chen, L.W., Long, R., Wu, M.M., Luo, D., 2012. A mechanical metamaterial made from a DNA hydrogel. Nat. Nanotechnol. 7 (12), 816–820.

Li, C.-Y., Zheng, B., Liu, Y.-H., Gao, J.-L., Zheng, M.-Q., Pang, D.-W., Tang, H.-W., 2020. A boosting upconversion luminescent resonance energy transfer and biomimetic periodic chip integrated CRISPR/Cas12a biosensor for functional DNA regulated transduction of non-nucleic acid targets. Biosens. Bioelectron. 169, 112650.

Li, H., Ma, Y., Fu, R., Peng, J., Zhai, Y., Li, J., Xu, W., Hu, S., Ma, H., Wheeler, A.R., 2024. Droplet-based microfluidics with mass spectrometry for microproteomics. Engineering 43, 37–53.

Li, S.-Y., Cheng, Q.-X., Wang, J.-M., Li, X.-Y., Zhang, Z.-L., Gao, S., Cao, R.-B., Zhao, G.-P., Wang, J., 2018. CRISPR-Cas12a-assisted nucleic acid detection. Cell Discov 4 (1), 20.

Li, Y., Zeng, R., Wang, W., Xu, J., Gong, H., Li, L., Li, M., Tang, D., 2022. Size-controlled engineering photoelectrochemical biosensor for human papillomavirus-16 based on CRISPR-Cas12a-induced disassembly of Z-scheme heterojunctions. ACS Sens. 7 (5), 1593–1601.

Liu, Q., Liu, M., Jin, Y., Li, B., 2022. Ratiometric fluorescent probe: a sensitive and reliable reporter for the CRISPR/Cas12a-based biosensing platform. Analyst 147 (11), 2567–2574.

Liu, Y., Chen, Y., Huang, S., Ma, X., Huang, X., Wang, X., Zhou, F., 2021. Rapid and sensitive diagnosis of drug-resistant FLT3-F691L mutation by CRISPR detection. Front. Mol. Biosci. 8.

Mao, Z., Deng, A., Jin, X., Zhou, T., Zhang, S., Li, M., Lv, W., Huang, L., Zhong, H., Wang, S., 2024. Highly specific and rapid multiplex identification of Candida species using digital microfluidics integrated with a semi-nested genoarray. Anal. Chem. 96 (47), 18797–18805.

Meng, Q., Wang, X., Wang, Y., Dang, L., Liu, X., Ma, X., Chi, T., Wang, X., Zhao, Q., Yang, G., 2021. Detection of the SARS-CoV-2 D614G mutation using engineered Cas12a guide RNA. Biotechnol. J. 16 (6), 2100040.

Qiu, Z., Shu, J., He, Y., Lin, Z., Zhang, K., Lv, S., Tang, D., 2017. CdTe/CdSe quantum dot-based fluorescent aptasensor with hemin/G-quadruplex DNzyme for sensitive detection of lysozyme using rolling circle amplification and strand hybridization. Biosens. Bioelectron. 87, 18–24.

Song, P., Chen, S.X., Yan, Y.H., Pinto, A., Cheng, L.Y., Dai, P., Patel, A.A., Zhang, D.Y., 2021. Selective multiplexed enrichment for the detection and quantitation of low-fraction DNA variants via low-depth sequencing. Nat. Biomed. Eng. 5 (7), 690–701.

Uhlmann, E., Ryte, A., Peyman, A., 1997. Studies on the mechanism of stabilization of partially phosphorothioated oligonucleotides against nucleolytic degradation. Antisense Nucleic Acid Drug Dev. 7 (4), 345–350.

Weng, Z., You, Z., Yang, J., Mohammad, N., Lin, M., Wei, Q., Gao, X., Zhang, Y., 2023. CRISPR-cas biochemistry and CRISPR-based molecular diagnostics. Angew. Chem. Int. Ed. 62 (17), e202214987.

Wu, X., Tay, J.K., Goh, C.K., Chan, C., Lee, Y.H., Springs, S.L., Wang, D.Y., Loh, K.S., Lu, T.K., Yu, H., 2021. Digital CRISPR-based method for the rapid detection and absolute quantification of nucleic acids. Biomaterials 274, 120876.

Yao, C., Zhang, R., Tang, J.P., Yang, D.Y., 2021. Rolling circle amplification (RCA)-based DNA hydrogel. Nat. Protoc. 16 (12), 5460–5483.

Zeng, R., Gong, H., Li, Y., Li, Y., Lin, W., Tang, D., Knopp, D., 2022. CRISPR-Cas12a-derived photoelectrochemical biosensor for point-of-care diagnosis of nucleic acid. Anal. Chem. 94 (20), 7442–7448.

Zeng, R., Wang, W., Chen, M., Wan, Q., Wang, C., Knopp, D., Tang, D., 2021. CRISPR-Cas12a-driven MXene-PEDOT: PSS piezoresistive wireless biosensor. Nano Energy 82, 105711.

Zhang, C., Cai, Z., Zhou, Z., Li, M., Hong, W., Zhou, W., Yu, D., Wei, P., He, J., Wang, Y., Huang, C., Wang, X., Wu, J., 2023. CASMART, a one-step CRISPR Cas12a-mediated isothermal amplification for rapid and high-resolution digital detection of rare mutant alleles. Biosens. Bioelectron. 222, 114956.

Zhang, K., Lv, S., Lin, Z., Li, M., Tang, D., 2018. Bio-bar-code-based photoelectrochemical immunoassay for sensitive detection of prostate-specific antigen using rolling circle amplification and enzymatic biocatalytic precipitation. Biosens. Bioelectron. 101, 159–166.

Zhang, Y., Wang, W., Zhou, X., Lin, H., Zhu, X., Lou, Y., Zheng, L., 2024. CRISPR-responsive RCA-based DNA hydrogel biosensing platform with customizable signal output for rapid and sensitive nucleic acid detection. Anal. Chem. 96 (40), 15998–16006.

Zhao, R., Tang, Y., Song, D., Liu, M., Li, B., 2023. CRISPR/Cas12a-Responsive hydrogels for conjugation-free and universal indicator release in colorimetric detection. Anal. Chem. 95 (50), 18522–18529.

Zhou, T., Fu, R., Hou, J., Yang, F., Chai, F., Mao, Z., Deng, A., Li, F., Guan, Y., Hu, H., 2024. Self-interference digital optofluidic genotyping for integrated and automated label-free pathogen detection. ACS Sens. 9 (12), 6411–6420.